

Tomographic Small-Animal Imaging Using a High-Resolution Semiconductor Camera

George A. Kastis, *Student Member, IEEE*, Max C. Wu, *Student Member, IEEE*, Steve J. Balzer, Donald W. Wilson, Lars R. Furenlid, *Member, IEEE*, Gail Stevenson, H. Bradford Barber, *Member, IEEE*, Harrison H. Barrett, *Senior Member, IEEE*, James M. Woolfenden, *Member, IEEE*, Patrick Kelly, and Michael Appleby

Abstract—We have developed a high-resolution, compact semiconductor camera for nuclear medicine applications. The modular unit has been used to obtain tomographic images of phantoms and mice. The system consists of a 64×64 CdZnTe detector array and a parallel-hole tungsten collimator mounted inside a $17 \text{ cm} \times 5.3 \text{ cm} \times 3.7 \text{ cm}$ tungsten–aluminum housing. The detector is a $2.5 \text{ cm} \times 2.5 \text{ cm} \times 0.15 \text{ cm}$ slab of CdZnTe connected to a 64×64 multiplexer readout via indium-bump bonding. The collimator is 7-mm thick, with a 0.38-mm pitch that matches the detector pixel pitch. We obtained a series of projections by rotating the object in front of the camera. The axis of rotation was vertical and about 1.5 cm away from the collimator face. Mouse holders were made out of acrylic plastic tubing to facilitate rotation and the administration of gas anesthetic. Acquisition times were varied from 60 to 90 s per image for a total of 60 projections at an equal spacing of 6° between projections. We present tomographic images of a line phantom and mouse bone scan and assess the properties of the system. The reconstructed images demonstrate spatial resolution on the order of 1 to 2 mm.

Index Terms—Biomedical imaging, Cadmium Zinc Telluride (CdZnTe), single photon emission computed tomography, small-animal imaging.

I. INTRODUCTION

IMAGING semiconductor detectors based on materials such as CdZnTe can possess excellent energy and spatial resolution and operate at noncryogenic temperatures. Such detectors can be used in biomedicine for high-resolution gamma-ray imaging of both humans and animals. Radiotracer imaging techniques in small animals can be useful in providing information on the progress of a disease and its treatment by allowing the animal to act as its own control. Several tomographic gamma-ray imaging systems using scintillators have recently been developed [1]–[4]. Semiconductor gamma-ray

imaging systems have also been constructed, but most of them have been used primarily for planar imaging [5], [6]. We have built a compact, high-resolution semiconductor imaging system using a high-resolution CdZnTe detector array and a parallel-hole collimator and, in collaboration with the University of California San Francisco, we have developed a procedure for acquiring tomographic images of small animals.

II. IMAGING METHODS

A. System Description

We have developed CdZnTe arrays for high-resolution imaging; details on design and construction of these pixel arrays have been reported elsewhere [7]–[9]. Briefly, these arrays consist of a $2.5 \text{ cm} \times 2.5 \text{ cm} \times 0.15 \text{ cm}$ slab of CdZnTe with a continuous gold electrode on the top and a 64×64 array of gold electrodes on the bottom. The continuous electrode is held at a constant bias of -140 V . The pixel size is $330 \mu\text{m}$ with interpixel separation of $50 \mu\text{m}$, resulting in a $380 \mu\text{m}$ pitch. Each pixel of the detector array is connected to a readout integrated circuit by an indium-bump bond. We designed a high-resolution parallel-hole collimator to match the pitch of the detector array. The collimator, fabricated by Tecomet, is a laminar composite of tungsten foils that have been etched in a square pattern using a photolithographic process. A similar manufacturing process has been used by other researchers in making high-resolution animal imaging systems [10], [11]. The performance of the collimator–detector combination as a planar imaging system has been investigated and reported elsewhere [5]. The prototype system is housed in a $25.4 \text{ cm} \times 15.6 \text{ cm} \times 5.2 \text{ cm}$ aluminum box with lead shielding surrounding the box. In this paper, we report on the tomographic performance of the prototype system as well as an improved version of its housing.

We designed a $17 \text{ cm} \times 5.3 \text{ cm} \times 3.7 \text{ cm}$ tungsten–aluminum housing to hold the CdZnTe detector array and tungsten collimator. This module forms a compact and portable imaging unit, and it is a large improvement over the bulky prototype system. The housing includes a thermoelectric cooler and signal-processing electronics. Details of the design and construction of this system have been presented elsewhere [12]. Imaging initially with the prototype, and ultimately the portable module, we obtained projections of a line phantom and mice by rotating them in front of the camera. We chose the axis of rotation to be vertical to eliminate gravitational movement of internal organs during imaging.

Manuscript received November 5, 2000; revised July 23, 2001. This work was supported by the National Institutes of Health under Grants RO1 CA75288 and P41 RR14304. G. Kastis is a scholar of the “Alexander S. Onassis” Public Benefit Foundation under Group-T040.

G. A. Kastis, S. J. Balzer, L. R. Furenlid, H. B. Barber, and H. H. Barrett are with the Department of Radiology, Division of Nuclear Medicine, University of Arizona, Tucson, AZ 85724 USA. They are also with the Optical Sciences Center, University of Arizona, Tucson, AZ 85721 USA.

D. W. Wilson, G. Stevenson, and J. M. Woolfenden are with the Department of Radiology, Division of Nuclear Medicine, University of Arizona, Tucson, AZ 85724 USA.

M. C. Wu is with the Joint Graduate Group in Bioengineering, University of California, Berkeley, CA 94720 USA. He is also with the Joint Graduate Group in Bioengineering, University of California, San Francisco, CA 94143 USA.

P. Kelly and M. Appleby are with Tecomet, Woburn, MA 01801 USA.

Publisher Item Identifier S 0018-9499(02)01674-X.

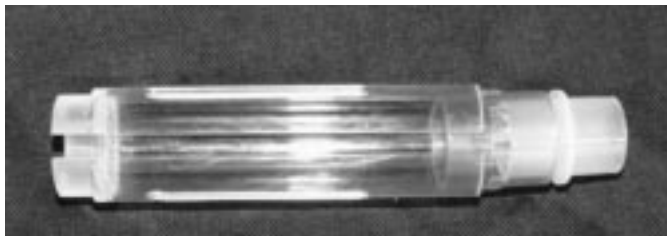


Fig. 1. Acrylic mouse holder resembling a rodent restrainer.

Mouse holders were made out of 1-in diameter acrylic tubing to facilitate imaging. A photo of our mouse holder is presented as Fig. 1. Similar holders have been developed by our collaborators at UCSF to facilitate ECG-gated myocardial imaging of small animals [13]. The mouse holders were fabricated to resemble commercially available cylindrical rodent restrainers. The mouse was gently pulled into the restrainer by its tail along the open groove until the animal was completely enclosed in the cylinder. A white Delrin nose piece placed up to the nose of the animal further confined any movement. An isoflurane/oxygen mixture was circulated via respiratory tubing inside the holder to provide anesthesia. An intravenous injection to the exposed tail-vein was performed after the animal was completely sedated. The holder was then attached to a precision rotational stage and placed with its center of rotation about 1.5 cm away from the face of the collimator. This was the closest distance from the center of rotation allowing the rotation stage to freely move over 360° .

The system setup including the animal holder and the portable imager, mounted on a set of translation stages, is shown in Fig. 2. A total of 60 projection images were collected for each object in 6° intervals. We restricted the acquisition time to 60–90 s/view. Each of the projections was corrected for activity decay. The field of view was limited by the size of the detector array to $2.5 \text{ cm} \times 2.5 \text{ cm}$. The overall collection efficiency of the detector-collimator system was about 1×10^{-5} . All of the tomographic images were generated using an maximum likelihood expectation maximization (ML-EM) iterative reconstruction algorithm, which corrects for the effects of collimator blur but not attenuation and scatter. The collimator blur was modeled geometrically and no other priors were applied. We used 100 iterations for reconstructing all images. Flood correction and median filtering were also applied to each of the projections to correct for inhomogeneities of the detector.

B. Line Phantom Imaging

A line phantom was made out of an acrylic rod to evaluate the resolution properties of our system. A diagram of this phantom is shown in Fig. 3. It consists of 15 2-mm diameter holes arranged in an equilateral triangular form. The center-to-center distance between holes was 4 mm. The line phantom was filled with 5 mCi of ^{99m}Tc aqueous solution and imaged for 1 minute over 60 views separated by 6° .

C. Animal Imaging

A 25 g mouse was injected with 18 mCi of ^{99m}Tc -methylene diphosphonate in the tail vein. A bone scan image of the skull and the thorax was acquired about three hours after injection. A

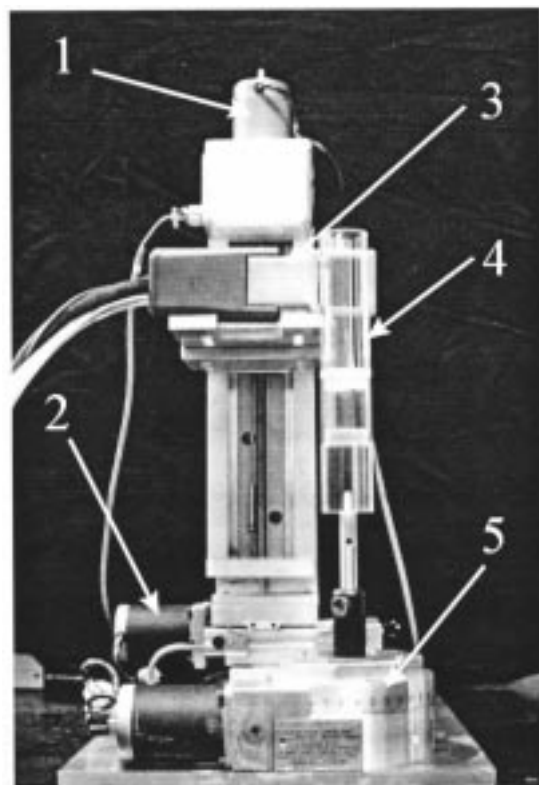


Fig. 2. Photograph of our imaging system composed of our portable gamma-ray imager (3) mounted on a set of translation stages (1 and 2). The animal holder (4) is attached on a rotation stage (5). Only the animal holder moves during image acquisition.

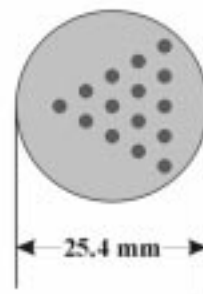


Fig. 3. Diagram of line phantom. The holes have a diameter of 2 mm and a center-to-center spacing of 4 mm.

0.5%–3% isoflurane/oxygen mixture was continuously administered into the holder keeping the animal completely sedated. The animal was monitored for depth of anesthesia. We obtained 60 projections with an acquisition time of 60 and 90 s/projection for the skull and thorax images, respectively.

III. RESULTS

A. Line Phantom

We assessed the resolution properties of the system by imaging the line phantom shown in Fig. 3. Fig. 4 shows a three-dimensional (3-D) visualization and a single slice of the reconstructed 60 projections of the line phantom. The 60 views were obtained with the portable unit. Individual lines are clearly resolved in the reconstructed image in Fig. 4. The

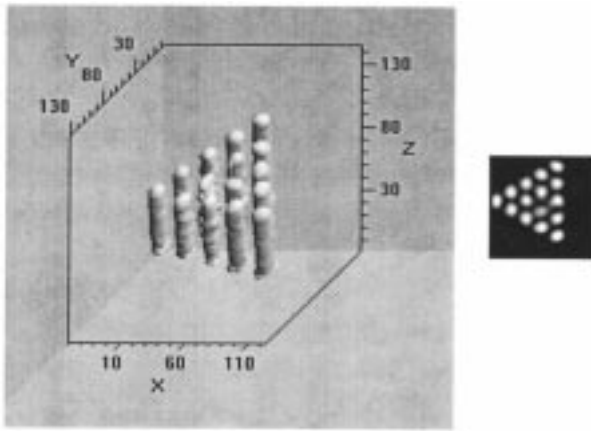


Fig. 4. Reconstructed image of the line phantom. (a) A single slice. (b) A 3-D visualization of the reconstructed image.

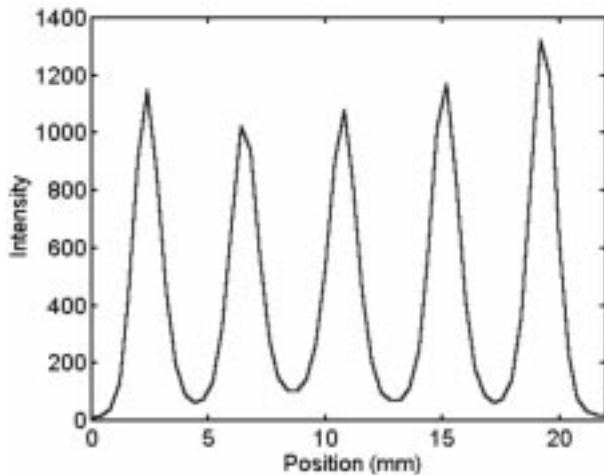


Fig. 5. Line profile of a representative slice showing clear separation of each line.

representative line profile in Fig. 5 shows a full-width at half maximum of about 2 mm. Since the holes were also 2 mm in diameter, it is very difficult to draw precise conclusion about spatial resolution from this image, but it is certainly of order 1–2 mm over the whole field.

B. Mouse Bone Scan

Tomographic images of a bone scan of the mouse thorax are shown in Fig. 6. Since our portable unit was not complete at this time these images were acquired with the prototype system. The set of images represents transverse slices of the thorax area with a 0.4 mm separation between slices. The mouse is oriented with its head to the right of the image. The front limbs and the outline of the thorax are clearly visible. Individual ribs can also be resolved.

Tomographic images of a bone scan of the mouse skull are shown in Figs. 7 and 8. Fig. 7 illustrates consecutive coronal slices of the skull while Fig. 8 shows consecutive transverse slices. The spacing between slices is 0.4 mm for both sequences. The images demonstrate anatomical features of the skull such as the zygomatic bones, the mandible, and the nasal turbinates with an estimated spatial resolution of 1 to 2 mm.

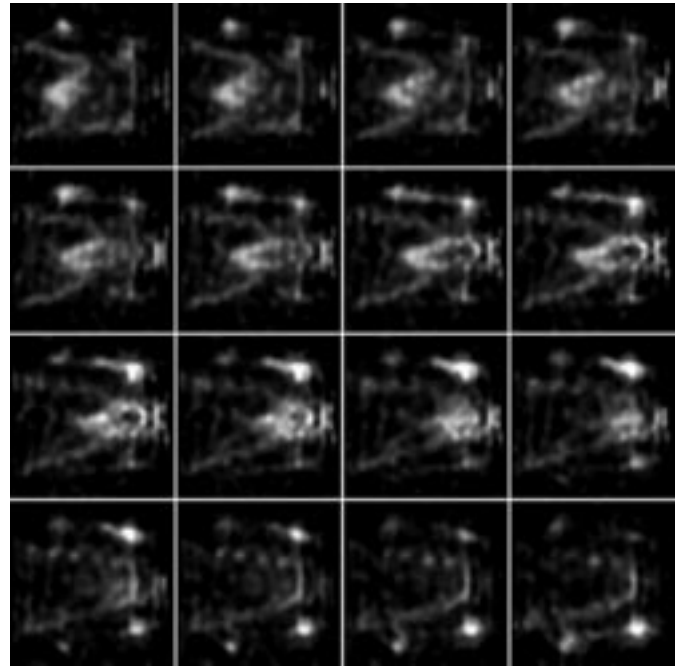


Fig. 6. Consecutive longitudinal slices of the bone scan of the thorax. The slices are oriented from dorsal to ventral with the animal's head pointing to the right of each slice.

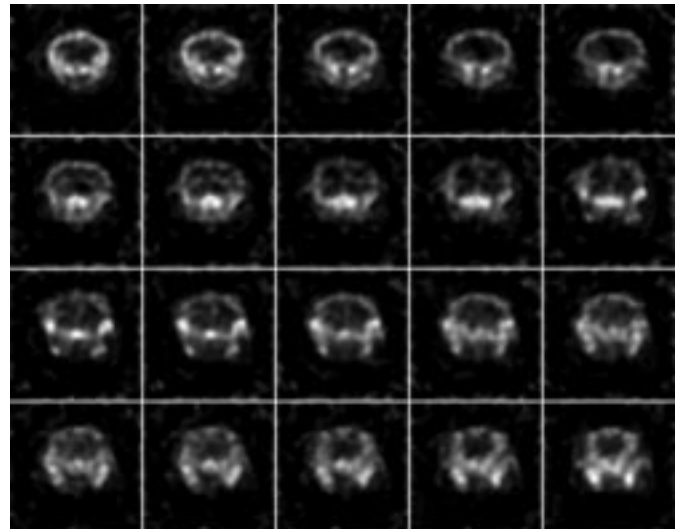


Fig. 7. Consecutive coronal slices of the bone scan of the mouse skull. The slices are oriented from caudal to rostral.

IV. DISCUSSION

We believe that our portable unit along with the rotation procedure can be very useful in a laboratory environment in acquiring tomographic images of small animals, primarily mice. The resolution of our system degrades linearly with the distance away from the collimator face. Fig. 9 illustrates the dependence of the calculated spatial resolution on the collimator-source distance. For larger objects one has to sacrifice resolution since larger holders and consequently greater detector-object distances are required. Furthermore, since the field of view of our system is limited to the size of the semiconductor array, larger objects can cause reconstruction artifacts when rotated in front of a small field-of-view camera.

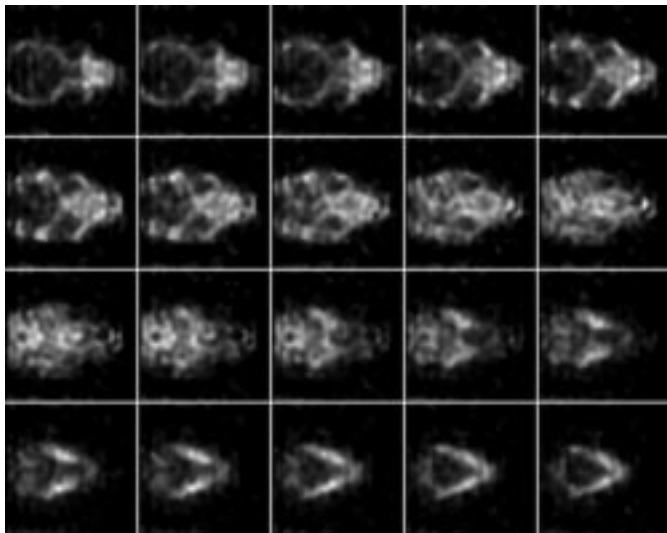


Fig. 8. Consecutive transverse slices of the bone scan of the mouse skull. The zygomatic arches and mandible can easily be resolved.

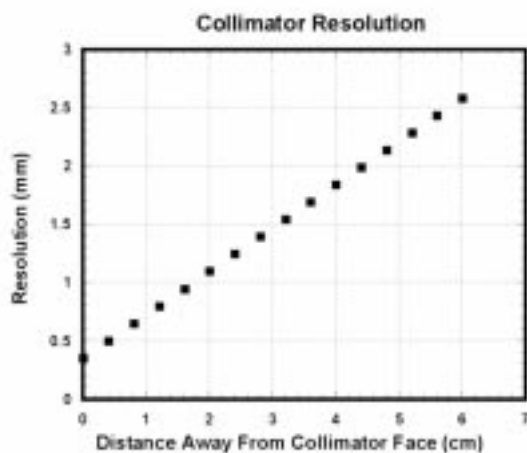


Fig. 9. Linear degradation of the calculated resolution of our system as a function of the source distance away from the collimator face.

The low sensitivity and consequently long acquisition times may appear to limit the use of this instrument in a commercial environment where high throughput of animals is usually required. However, in this case multiple modules can be used to reduce the necessary projections and acquisition time. Four modules placed in a square pattern can be a feasible arrangement keeping the collimator-object distance minimal. However, in order to fit more than four cameras a larger distance is required and consequently a sacrifice in resolution. Furthermore, one is also limited by the time it takes to sedate the animal as well as the recovery time. Isoflurane allows for both a rapid induction and recovery.

V. CONCLUSION

We have demonstrated that high-resolution tomographic images of mice can be acquired using a collimated CdZnTe imaging array. By rotating the object in front of the camera,

we obtained images of a line phantom and a mouse bone scan with 1–2 mm spatial resolution. The field of view was limited to 2.5 cm \times 2.5 cm due to the size of the semiconductor array. We are presently constructing tomographic imaging systems with multiple imaging modules that will provide a larger field of view and shorter acquisition times.

ACKNOWLEDGMENT

The authors would like to thank G. McNeill and the technical staff of the Division of Nuclear Medicine of University Medical Center at the University of Arizona for support with the radiotracers. They would like to further thank B. Skovan for her assistance.

REFERENCES

- [1] S. R. Cherry, Y. Shao, R. W. Silverman, K. Meadors, S. Siegel, A. Chatziioannou, J. W. Young, W. Jones, J. C. Moyers, D. Newport, A. Bouf-nouchet, T. H. Farquhar, M. Andreaco, M. J. Paulus, D. M. Binkley, R. Nutt, and M. E. Phelps, "MicroPET: A high resolution PET scanner for imaging small animals," *IEEE Trans. Nucl. Sci.*, vol. 44, pp. 1161–1166, June 1997.
- [2] G. K. Kastis, H. B. Barber, H. H. Barrett, H. C. Gifford, I. W. Pang, D. D. Patton, J. D. Sain, G. Stevenson, and D. W. Wilson, "High-resolution SPECT imager for three-dimensional imaging of small animals," *J. Nucl. Med.*, vol. 39, no. 5(suppl.), p. 9P, May 1998.
- [3] A. P. Jeavons, R. A. Chandler, and C. A. R. Dettmar, "A 3-D HIDAC-PET camera with submillimeter resolution for imaging small animals," *IEEE Trans. Nucl. Sci.*, vol. 46, pp. 468–473, June 1999.
- [4] N. Schramm, A. Wirrwar, F. Sonnenberg, and H. Halling, "Compact high resolution detector for small animal SPECT," *IEEE Trans. Nucl. Sci.*, vol. 47, pp. 1163–1167, June 2000.
- [5] G. A. Kastis, H. B. Barber, H. H. Barrett, S. J. Balzer, D. Lu, D. G. Marks, G. Stevenson, J. M. Woolfenden, M. Appleby, and J. Tueller, "Gamma-ray imaging using a CdZnTe pixel array and a high-resolution, parallel-hole collimator," *IEEE Trans. Nucl. Sci.*, vol. 47, pp. 1923–1927, Dec. 2000.
- [6] C. Scheiber, B. Eclancher, J. Chambron, V. Prat, A. Kazandjan, A. Jahnke, R. Matz, S. Thomas, S. Warren, M. Hage-Hali, R. Regal, P. Siffert, and M. Karman, "Heart imaging by cadmium telluride gamma camera European Program 'BIOMED' consortium," *Nucl. Instrum. Meth. Phys. Res. A*, vol. 428, no. 1, pp. 138–149, 1999.
- [7] K. J. Matherson, H. B. Barber, H. H. Barrett, J. D. Eskin, E. L. Dereniak, D. G. Marks, J. M. Woolfenden, E. T. Young, and F. L. Augustine, "Progress in the development of large-area modular 64 \times 64 CdZnTe imaging arrays for nuclear medicine," *IEEE Trans. Nucl. Sci.*, vol. 45, pp. 354–358, June 1998.
- [8] H. B. Barber, H. H. Barrett, F. L. Augustine, W. J. Hamilton, B. A. Apotovsky, E. L. Dereniak, F. P. Doty, J. D. Eskin, J. P. Garcia, D. G. Marks, K. J. Matherson, J. M. Woolfenden, and E. T. Young, "Development of a 64 \times 64 CdZnTe array and associated readout integrated circuit for use in nuclear medicine," *J. Electron. Mater.*, vol. 26, no. 6, pp. 765–772, 1997.
- [9] J. M. Woolfenden, H. B. Barber, H. H. Barrett, E. L. Dereniak, J. D. Eskin, D. G. Marks, K. J. Matherson, E. T. Young, and F. L. Augustine, "Modular 64 \times 64 CdZnTe arrays with multiplexer readout for high-resolution nuclear medicine imaging. 'Semiconductors for room-temperature radiation detector applications II,'" in *Proc. Mat. Res. Soc. Symp.*, vol. 487, R. B. James, Ed., Boston, MA, Dec. 1997, pp. 239–243.
- [10] A. Valda Ochoa, L. Ploux, R. Mastroppolito, Y. Charon, P. Lanièce, L. Pinot, and L. Valentin, "An original emission tomograph for *in vivo* brain imaging of small animals," *IEEE Trans. Nucl. Sci.*, vol. 44, pp. 1533–1537, Aug. 1997.
- [11] L. Ploux, R. Mastroppolito, L. Pinot, P. Lanièce, Y. Charon, A. Valda Ochoa, and L. Valentin, "TOHR: Prototype design and characterization of an original small animal tomograph," in *Proc. Conf. Record IEEE Nuclear Science Symp.*, vol. 2, Albuquerque, NM, Nov. 1997, pp. 1063–1067.
- [12] S. J. Balzer, "A portable gamma-ray imager for small animal studies," M.S. thesis, Univ. Arizona, Tucson, 2000.
- [13] M. C. Wu, H. R. Tang, D. W. Gao, A. Ido, J. W. O'Connell, B. H. Hasegawa, and M. W. Dae, "ECG-Gated pinhole SPECT in mice," *IEEE Trans. Nucl. Sci.*, vol. 47, pp. 1218–1221, June 2000.